

Analytical approximation for the structure of differentially rotating barotropes

A. Odrzywołek[?]

Institute of Physics, Jagiellonian University, Reymonta 4, 30-059 Krakow, Poland

Released 2003 May 18

ABSTRACT

Approximate analytical formula for density distribution in differentially rotating stars is derived. Any barotropic EOS and conservative rotation law can be handled with use of this method for wide range of differential rotation strength. Results are in good qualitative agreement with comparison to the other methods. Some applications are suggested and possible improvements of the formula are discussed.

Key words: stars: rotation – methods: analytical

1 INTRODUCTION

Theory of self-gravitating rotating bodies seems to be an unlimited reservoir of difficult problems hardly tractable even under severe simplifications. It is a subject of scientific effort since 1742 when Maclaurin has initiated this field by his studies on incompressible rotating ellipsoids (Maclaurin 1742). Development of modern numerical calculations resulted in progress in practical applications nowadays such as e.g. 3D hydrodynamical simulations of rotation of complex objects.

Analytical approach has succeeded for constant density, incompressible bodies. Work of Maclaurin, Jacobi, Poincare, Schwarzschild and many others has explained the behaviour of those objects almost completely (Lyttleton 1953). Behaviour of slowly rotating polytropes has been calculated by Chandrasekhar (1936). By applying the differential equation of hydrostatical equilibrium modified by rotation he reduced the problem to an ordinary differential equation. This method however works only for a uniform rotation. This list would be incomplete without the Roche model. It's simplicity makes it a very powerful tool for understanding behaviour of rotating objects. Present computational methods allow one to handle numerically two- and three-dimensional problems with complicated governing equations

In this paper we present simple analytical approach which can treat differentially rotating compressible barotropic stars in case of slow or moderately fast rotation. This model could fill a gap between simple analytical methods used for e.g. Maclaurin spheroids or Roche model, and complicated numerical methods such as e.g. HSCF (Hachisu 1986), or those applying straightforward Newton-Raphson technique (Eriguchi & Müller 1985).

2 FORMULATION OF THE PROBLEM

We attempt to find a density distribution (iso-density contours) of a single self-gravitating object under the following assumptions:

- (i) Barotropic EOS $p = p(\rho)$
- (ii) Simple rotation $\mathbf{v} = \boldsymbol{\omega} \times \mathbf{r}$ with angular velocity dependent only on the distance from rotation axis $\omega = \omega(r)$
- (iii) Newtonian gravity
- (iv) Axisymmetric density distribution
- (v) We seek solutions for stationary objects in full mechanical equilibrium, i.e. all quantities are time-independent

With properties (i)–(v) satisfied, the Euler equation becomes, in cylindrical coordinates (r, z, ϕ) :

$$r \frac{d}{dr} \left(\frac{1}{r} \frac{dp}{dr} + r \frac{d\omega}{dr} \right) = 0 \quad (1)$$

Continuity equation is then fulfilled automatically. Introducing centrifugal potential:

$$\phi_c(r) = \int_0^r \omega^2(r') r' dr' \quad (2)$$

and enthalpy:

$$h(\rho) = \int \frac{1}{\rho} d\rho \quad (3)$$

we get a simple equation:

$$r [h(\rho) + \phi_g + \phi_c] = 0 \quad (4)$$

with a solution

$$h(\rho) + \phi_g + \phi_c = C = \text{const} \quad (5)$$

Equation (5) is the most important equation in the study of the structure of rotating stars under conditions (i)–(v). We define the integration constant in eq. (3) to be such that the enthalpy satisfies the condition $h(\rho = 0) = 0$. The only term which we haven't

[?] E-mail: odrzywolek@th.if.uj.edu.pl

specified yet is the gravitational potential ϕ . If we use the Poisson equation:

$$\nabla^2 \phi = 4\pi G \rho \quad (6)$$

where G is the gravitational constant, the equation (5) becomes a non-linear second-order differential equation. This form, however, is very inconvenient, because we have to specify boundary conditions at a surface of the star,¹ which is unknown *a priori*. More powerful is an integral form of eq. (5) obtained by substitution:

$$\phi(r) = -G \int \frac{\rho(r')}{|r-r'|} d^3x' \quad (7)$$

This integral form has been used in very successful numerical algorithm developed originally by Ostriker & Mark (1968), and recently improved by Hachisu (1986) and by Eriguchi & Müller (1985). This form will be also used to derive our approximation formula in the next section.

3 APPROXIMATION FOR THE DENSITY DISTRIBUTION

The *integral equation* form of eq. (5) is:

$$h(r) + R(\rho) + \frac{1}{2}\Omega^2 r^2 = C \quad (8)$$

where R is the integral operator acting on the density performing the integration on the right-hand side of eq. (7) over entire volume of the star. We define the surface of the star to be manifold consisting of points where $\rho = 0$, $h = 0$. Explicit form of the operator R in terms of coordinates will not be needed. For a given EOS and for a fixed rotation law i.e. for given functions $h(r)$ and Ω , the only free parameter is the constant C . The values of C label a family of the stellar models with the same EOS and rotation pattern, which differ in total mass and maximum density² etc.

Eq. (8) has a form of the Hammerstein non-linear integral equation (Hammerstein 1930) and can be rewritten in a canonical form:

$$f = R[F(f)] \quad (9)$$

where:

$$f = C - \frac{1}{2}\Omega^2 r^2 - h(r); \quad F(f) = h^{-1}(f + \frac{1}{2}\Omega^2 r^2 - C) \quad (10)$$

In case of linear function F , eq. (9) could be easily solved by the von Neumann series. This strongly suggests to try the following iteration scheme:

$$f_1 = R[F(f_0)];$$

$$f_2 = R[F(f_1)];$$

$$f_n = R[F(f_{n-1})]$$

Indeed, an iteration procedure of this type was successfully applied in the so-called self-consistent field method (Ostriker & Mark

¹ The fact of the surface of non-rotating stars is spherical allows us to specify boundary conditions with one real number – the radius. Generally, in rotating objects we have a surface represented by some function of two variables which has to be determined.

² In differentially rotating stars the central density may be, but generally is not, the maximum density.

1968, Hachisu 1986). We have introduced the canonical form to ensure that the first-order approximation is found in a correct order i.e. by using the first line of the sequence (11). When we go back to non-canonical form (8) the first line of (11) takes the form:

$$C - \frac{1}{2}\Omega^2 r^2 - h(r) = R(\rho) \quad (12)$$

From eq. (12) above we can find the first-order deviation from sphericity. It seems impossible at first sight to avoid explicit integration in eq. (12). In case of a general Ω , this is true. But let us look at equation (8) in case of vanishing centrifugal potential $\frac{1}{2}\Omega^2 r^2$, i.e. with no rotation:

$$h(r) + R(\rho) = C \quad (13)$$

When we use a function which satisfies eq. (13) as zero-order approximation:

$$h(r_0) + R(\rho_0) = C_0 \quad (14)$$

integration in eq. (12) can be easily eliminated:

$$C - \frac{1}{2}\Omega^2 r^2 - h(r) = R(\rho) = C_0 - h(r_0) \quad (15)$$

Finally, our formula takes the form:

$$h(r_1) = h(r_0) - \frac{1}{2}\Omega^2 r^2 + C - C_0 \quad (16)$$

or simpler, using the enthalpy ($h(r_0) = h_0$, $h(r_1) = h_1$):

$$h_1 = h_0 - \frac{1}{2}\Omega^2 r^2 + C - C_0 \quad (17)$$

Functions used as zero-order approximation (ρ_0 or h_0) are simply density and enthalpy distributions of non-rotating barotropic stars. In case of polytropic EOS, $p = K\rho^\gamma$, these quantities are given by Lane-Emden functions. In more general case we have to find solution of the ordinary differential equation of the hydrostatic equilibrium.

The only unanswered question is what are the value of constants C and C_0 ³. It is an essential part of this work, so we decided to explain it in a separate section.

4 ADJUSTING CONSTANTS

When we try to find the enthalpy distribution using the formula (17) we have to find the best zero-order function h_0 and the value of C_0 given by h_0 . An equivalent problem is to find the equation for which the function h_0 and the value C_0 are best zero-order approximations – in this case we seek for C . We consider the latter case, as we have to find only one real number. Let us denote:

$$C = C_0 - C : \quad (18)$$

In our approximation, the equation for the first-order enthalpy distribution h_1 , in terms of the initial spherical distribution h_0 and (11) rotation law is, from (17):

$$h_1 = h_0 - \frac{1}{2}\Omega^2 r^2 + C \quad (19)$$

where C is still to be determined.

The terms in eq. (19) behave as follows:

(i) ‘ h_0 ’ is spherical enthalpy distribution, thus it is only a function of the radius, has a maximum at the centre, and goes monotonically to zero, where usually is cut. However, from mathematical point of view, Lane-Emden functions extend beyond the first zero point with negative function values.

³ For a given EOS the function ρ_0 gives C_0 and *vice versa*.

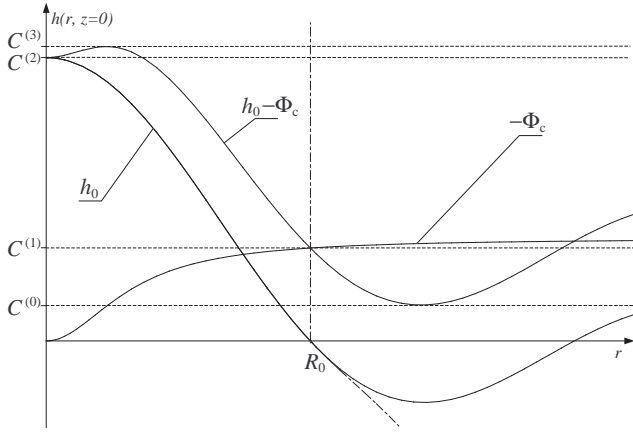


Figure 1. Schematic graphs of the two first terms in eq. (19), explaining the meaning of C . The most general case is shown. In some particular cases $C^{(0)}$ and $C^{(2)}$ may not exist – this depends on the both h_0 and Φ_c . Vertical dot-dashed line shows that $C^{(1)} = \Phi_c(R_0)$, where R_0 is radius of non-rotating star. The dashed curve fragment below the axis reflects ambiguity of the Lane-Emden function continuation to negative values, as described in the text. This figure prepared with use of eq. (40) for $z = 0$.

(ii) ‘ Φ_c ’ is a monotonically increasing function of distance from the rotation axis. It starts with zero at the rotation axis. It does not change the enthalpy along the axis of symmetry. The strongest enthalpy increase takes place along the equatorial plane.

(iii) ‘ C ’ shifts the sum of positive functions h_0 and Φ_c down.

At first sight, shifting down by C seems not needed (i.e. one would adopt $C = 0$), because we obtain correct qualitative behaviour – the star is expanded along equator. But often it is enough to introduce slow rotation to get positive value of $h_0 - \Phi_c$ (i.e. for our approximation to the enthalpy in this case) for any $r > 0; z = 0$ i.e. equatorial radius becomes infinite. It leads directly to physically unacceptable results – infinite volume and mass. So the value C plays a non-trivial role and has to be found. Fig. 1 shows the behaviour of all terms in eq. (19) along the equator of the star, where the rotation acts most strongly. Horizontal lines show points where enthalpy is cut for a given value of C .

We can distinguish some important values:

(i) For $C < C^{(0)}$ we obtain infinite radius of a star. These values obviously have to be rejected.

(ii) For $C^{(0)} < C < C^{(1)} = \Phi_c(R_0)$, where R_0 is the radius of a zero-order density distribution, we get finite volume of a star, but we use extension of h_0 with negative values. This introduces some problems which we discuss later in the article, although the resulting enthalpy and density are positive and physically acceptable.

(iii) For $C^{(1)} < C < C^{(2)} = h_0(r=0; z=0)$ we get a density distribution which is topologically equivalent to the ball.

(iv) For $C^{(2)} < C < C^{(3)} = (h_0 - \Phi_c)_{\max}$ we get toroidal density distribution. This case exists only if strong differential rotation is present.

(v) For $C > C^{(3)}$ the star disappears.

We expect to find the solution in the range $C^{(0)} < C < C^{(2)}$ because we are looking for finite-volume non-toroidal stars.

One can try to find C both analytically and numerically. To keep the algebraic form and the simplicity of the formula, we now concentrate on the former method.

When we substitute the formula (19) into our basic equation (5) we get:

$$h_0 - C + C_0 + \Phi_c(r_1) + \Phi_c = C \quad (20)$$

In this formula we have made use of (18). After obvious simplifications, using (14) and denoting $R(r_0) = \Phi_c(r_0)$ we have:

$$\Phi_c(r_1) = \Phi_c(r_0) \quad (21)$$

This equality is true only if $r_0 = r_1$. The same holds for the enthalpy:

$$h_1 = h_0: \quad (22)$$

Using formula (19) again we finally obtain:

$$C = \Phi_c \quad (23)$$

Left-hand side of eq. (23) is constant, while the right-hand side is a function of distance from the rotation axis, monotonically decreasing from zero. This equality holds only in trivial case $C = 0$ and $\Phi_c = 0$ with no rotation at all. In any other case (23) cannot be fulfilled. So instead we try another possibility and require that

$$C = \Phi_c \quad (24)$$

where ‘hat’ denotes some mean value of the function Φ_c . We have chosen

$$C = \Phi_c = \frac{4}{3} R_0^3 \int_0^Z \Phi_c^3 r \, dz \quad (25)$$

Integration is taken over the entire volume $V_0 = \frac{4}{3} R_0^3$ of a non-rotating initial star with the radius R_0 . This choice of C gives good results. But using the mean value theorem:

$$\int_0^Z \Phi_c^3 r \, dz = V_0 \Phi_c; \quad (26)$$

where Φ_c is some value of Φ_c in the integration area, and taking in account monotonicity of the centrifugal potential $0 < \Phi_c < \Phi_c(R_0)$ we get:

$$C = \Phi_c < \Phi_c(R_0) \quad (27)$$

i.e. the value of C is in the range $C < C^{(1)}$ from Fig. 1. It forces us to use negative values of non-rotating enthalpy. Moreover, in case of polytropic EOS with fractional polytropic index⁴ Lane-Emden equation (Kippenhahn & Weigert 1994):

$$\frac{1}{z^2} \frac{d}{dz} \left(z^2 \frac{dw}{dz} \right) + w^n = 0 \quad (28)$$

has no real negative values, because of fractional power of negative term w^n . But we can easily write equation, with solution identically equal to solution of Lane-Emden equation for $w > 0$, and real solution for $w < 0$ e.g.:

$$\frac{1}{z^2} \frac{d}{dz} \left(z^2 \frac{dw}{dz} \right) + j w^j = 0 \quad (29)$$

But, for example, solution of the following equation:

$$\frac{1}{z^2} \frac{d}{dz} \left(z^2 \frac{dw}{dz} \right) + \frac{j w^{j+1}}{w} = 0 \quad (30)$$

is again identically equal to solution of Lane-Emden equation for

⁴ Physically interesting cases like degenerate electron gas in non-relativistic case has fractional polytropic index $n = 3/2$.

$w > 0$, but differs from eq. (29) for $w < 0$. Fortunately, difference between solution of eq. (29) (Fig. 1, below axis, dot-dashed) and eq. (30) (Fig. 1, solid) for $w < 0$ is small if $j \ll 1$. Example from Fig. 1 (for $n = 1$) is representative for other values of n . We will use form (29) instead of the original Lane-Emden equation (28) for calculations in this article.

To avoid problems with negative enthalpy we can put simply:

$$C = c(R_0) \quad (31)$$

which is strictly boundary value $C^{(1)}$ from Fig. 1. The great advantage of the eq. (31) is the possibility to analytically perform the integration of the centrifugal potential (2) for most often used forms of $\omega(r)$. In contrast, in formula (25), not only angular velocity profile (2), but also the centrifugal potential have to be analytically integrable function. In both cases (25, 31) however, possibility of analytical integration depends on the form of $\omega(r)$. The value of C from eq. (31) also gives reasonable iso-density contours, cf. Fig. 11 and 8, but global accuracy is poor (Table 1).

As we noticed, the best value of C in formula (19) could be found numerically. For example, we can use virial theorem formula for rotating stars (cf. Tassoul 2000):

$$2E_k - E_g + 3 \int_0^1 \rho d^3 r = 0; \quad (32)$$

where E_k and E_g is the rotational kinetic energy and the gravitational energy, respectively. We define, so-called virial test parameter Z :

$$Z = \frac{2E_k - E_g + 3 \int_0^1 \rho d^3 r}{E_g} \quad (33)$$

where we introduced internal energy:

$$U = \frac{1}{2} \int_0^1 \rho d^3 r \quad (34)$$

Parameter Z is very common test of the global accuracy for rotating stars models. We may request that our enthalpy satisfy (32), i.e. we choose C from equation:

$$Z(h_0, c, C) = 0 \quad (35)$$

We can find C from equation eq. (35) numerically only.

As it is shown on Fig. 2, we can find approximation of the rotating polytrope structure in form (19) satisfying virial theorem (32) up to accuracy limited only by numerical precision.

Values of C obtained with (31), (25) and from virial test (35) are compared on Fig. 3. Some of the global model properties are very sensitive to value of C (cf. Figs 2 and 5).

Because virial test is unable to check accuracy of our model, we may also try to compare directly eq. (19) with enthalpy distribution from the numerical calculations h_{num} of e.g. Hachisu (1986), Eriguchi & Müller (1985) and find C minimizing e.g. the following formula:

$$\int_0^1 |h_1(C) - h_{\text{num}}|^2 d^3 r = \min \quad (36)$$

This method however, requires numerical results (e.g. enthalpy distribution) in machine-readable form.

5 APPROXIMATE FORMULA ACCURACY

In the above sections, we tried to be as general as possible. Now we give some examples, and test accuracy of approximation.

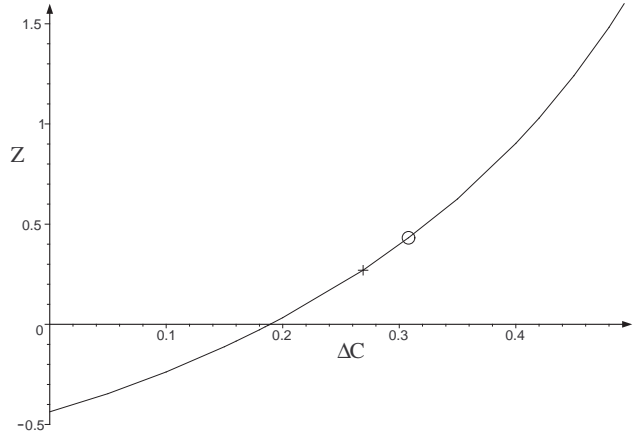


Figure 2. Behaviour of virial test parameter Z vs C for $n = 3=2$ polytropic model (41) with j -const angular velocity profile for $\omega_0 = 1.5$ and $A = 0.2R_0$. Proper choice of C can give density distribution satisfying virial theorem to arbitrary accuracy. $C = 0.308$ from eq. (31) is represented by circle. Cross marks value $C = 0.269$ given by formula (25). Virial theorem will be satisfied when we take C , given by intersection of Z with horizontal axis i.e. $C = 0.189$.

In case of polytropic EOS $p = K \rho^{1/n}$ the enthalpy is:

$$h(r) = \frac{K}{1-n} \rho^{1/n} \quad (37)$$

Zero-order approximation of density (density of non-rotating polytrope, Kippenhahn & Weigert 1994) with n -th⁵ Lane-Emden function w_n is:

$$\rho = c [w_n(Ar)]^n; \quad A^2 = \frac{4G}{nK} \frac{\rho_0^{n-1}}{c} \quad (38)$$

and our formula for density becomes:

$$\rho = c^{1-n} w_n \left(\frac{1}{nK} (c + C) \right)^n \quad (39)$$

where C is calculated from (25), (31) or (35).

In certain cases Lane-Emden functions are elementary functions as e.g. w_1 . In cases like this our formula may be expressed even by elementary functions. For example, for $n = 1$, $K = 1=2$, $4G = 1$, $c = 1$, $\omega(r) = \omega_0 = (1 + r^2 = A^2)$ and C from eq. (31) we get a simple formula:

$$\rho(r; z) = \frac{\sin^2 \left(\frac{r^2 + z^2}{2} \right)}{r^2 + z^2} + \frac{1}{2} \frac{A^2 r^2}{1 + r^2 = A^2} + \frac{1}{2} \frac{A^2 z^2}{1 + z^2 = A^2} \quad (40)$$

Functions like this can easily be visualized on a 2D plot. Figure 1 has been made from the formula (40) while figures 8 and 11 from eq. (41).

Now we concentrate on $n = 3=2$ polytrope. In our calculations and figures we will use $4G = 1$, $c = 1$ and $K = 2=5$. Now formula (39) becomes:

$$\rho = (w_n c + C)^{3=2} \quad (41)$$

Iso-density contours of ρ from (41) are presented on Fig. 11 and Fig. 8.

To test accuracy of approximation we have calculated axis ratio, total energy, kinetic to gravitational energy ratio, and dimensionless angular momentum. Axis ratio is defined as usual as:

$$\text{Axis Ratio} = \frac{R_z}{R_{\text{eq}}} \quad (42)$$

$$j = 1 + \frac{1}{n}$$

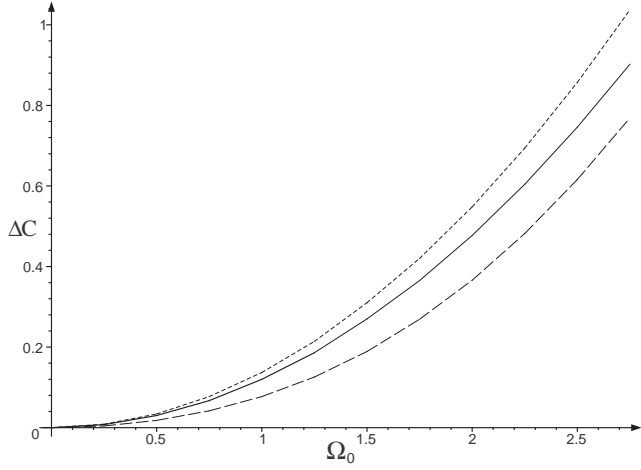


Figure 3. Dependence of ΔC on Ω_0 , given by eq. (31) (dotted), calculated from (25) (solid) and given by virial theorem constrain (35) (dashed). Both values estimated by (25, 35) are below $\Delta C = \Delta C_c(R_0)$ i.e. $\Delta C^{(1)}$ from Fig. 1. It shows, that continuation of Lane-Emden equation to negative values is required for successful approximation of the rotating body structure. Density distribution was given by eq. (41) with j -const angular velocity with $A = 0.2R_0$.

where R_z is distance from centre to pole and R_{eq} is equatorial radius. Total energy E_{tot} :

$$E_{tot} = (E_k + E_g + U) = E_0 \quad (43)$$

is normalized by:

$$E_0 = (4G)^2 \frac{M^5}{J^2} \quad (44)$$

and dimensionless angular momentum is defined as:

$$j^2 = \frac{1}{4} \frac{J^2}{GM^{10/3}} \frac{1=3}{m_{ax}} \quad (45)$$

where M and J are total mass and angular momentum, respectively; m_{ax} is maximum density. Quantities (42)-(45) are computed numerically from (41), with given angular velocity (Ω) and chosen ΔC .

5.1 Influence of ΔC

We have made detailed comparison of our $n = 3=2$ model (41) with j -const rotation law and $A = 0.2R_0$ (middle row of Fig. 8) for different values of ΔC with results of (Eriguchi & Müller 1985, Table 1b). Table 1 show our results for ΔC from eq. (25). Value of ΔC from eq. (31) and corresponding virial test parameter Z is included here for comparison. Table 2 shows global properties of our approximation with ΔC equal to the solution of eq. (35), i.e. satisfying virial theorem.

Direct comparison of values from Table 1 and table Table 2 to Table 1b of Eriguchi & Müller (1985) may be difficult, because our driving parameter is central angular velocity Ω , while Eriguchi & Müller (1985), following successful approach of Hachisu (1986), use axis ratio (42). More convenient in this case is comparison of figures prepared from data found in Table 1b of Eriguchi & Müller (1985) and our tables. This is especially true, because axis ratio isn't well predicted by our formula (cf. Fig. 6 and Fig. 7), while global properties (E_{tot} , j^2 , $E_k = \mathcal{E}_g j$ cf. Fig. 4, 5) and virial test Z are in good agreement if $E_k = \mathcal{E}_g j$ ≈ 0.1 .

Fig. 4 shows that our approximation is valid until $E_k = \mathcal{E}_g j$

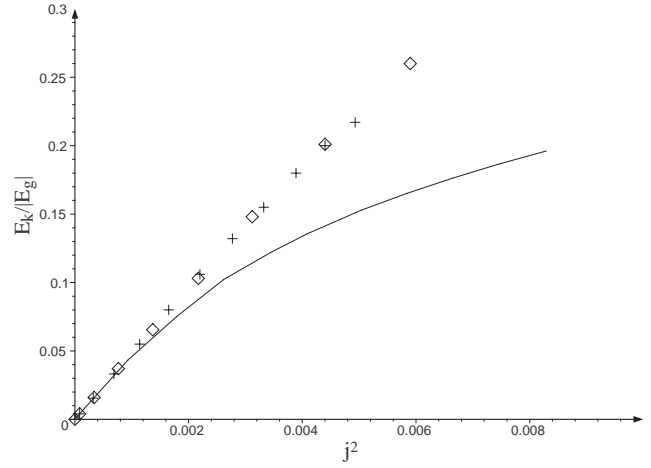


Figure 4. $E_k = \mathcal{E}_g j$ ratio as a function of the square of dimensionless angular momentum j^2 for our model (41) with $n = 3=2$, $\Omega_0 = 1.5$ and $A = 0.2R_0$. Solid line represent numerical results of (Eriguchi & Müller 1985). We see that our formula behaviour is in good agreement with numerical results if $E_k = \mathcal{E}_g j \approx 0.1$. Results using ΔC from eq. (25) are marked by crosses. Results satisfying virial theorem (ΔC from eq. (35)) are represented by diamonds. As it is apparent from figure above, ΔC has no influence on this relation, and can't improve accuracy of the formula (17).

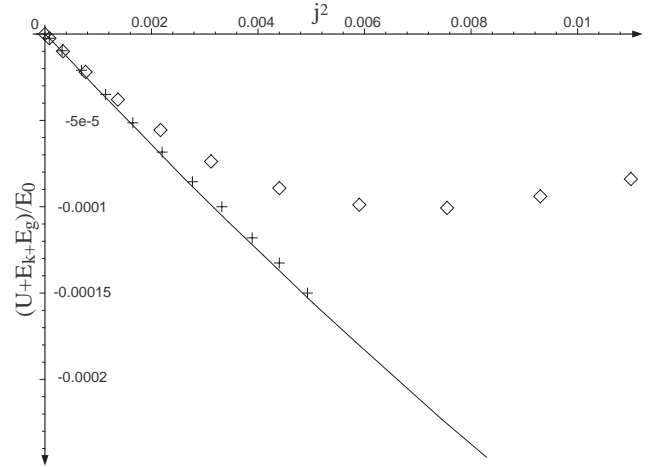


Figure 5. Total energy versus j^2 . We can see great improvement of results with ΔC from eq. (35) marked by '+'. ΔC from eq. (25) (◇) gives incorrect behaviour of the total energy. Solid line represent results of Eriguchi & Müller (1985), cross and diamonds are result derived from our approximate formula (41) with ΔC from virial test (35) and eq. (25), respectively. Approximation satisfying virial equation gives results resembling numerical calculations. Parameters of model are given in caption of Fig. 4.

≈ 0.1 , and begins to diverge from numerical results strongly for $E_k = \mathcal{E}_g j > 0.1$. Both values of ΔC (25,35) give similar behavior here. However, ΔC from virial test produces better results, and $E_k = \mathcal{E}_g j$ values are more sensible for the strongest rotation.

In contrast, total energy (43) is very sensitive to ΔC . Value of ΔC from eq. (25) produces wrong result. E_{tot} begin to increase for $j^2 > 0.007$, while numerical results give monotonically decreasing E_{tot} . Use of ΔC from (35) instead, gives correct result, cf. Fig. 5.

While global properties of our model are in good agreement with numerical results for $E_k = \mathcal{E}_g j \approx 0.1$, axis ratio tends to be

| α | Axis Ratio | j^2 | $\frac{E_k}{E_g j}$ | $\frac{E_g + E_k + U}{E_0}$ | Virial test Z | \mathcal{F} | C | \mathcal{C} | | |
|----------|------------|-------|---------------------|-----------------------------|---------------|---------------|------|---------------|------|------|
| 0.25 | 1.01 | 8.41 | 10^{-5} | 0.004 | 2.50 | 10^{-6} | 0.01 | 0.01 | 0.01 | 0.01 |
| 0.50 | 1.05 | 3.38 | 10^{-4} | 0.02 | 1.00 | 10^{-5} | 0.03 | 0.04 | 0.03 | 0.03 |
| 0.75 | 1.15 | 7.64 | 10^{-4} | 0.04 | 2.20 | 10^{-5} | 0.07 | 0.10 | 0.07 | 0.08 |
| 1.00 | 1.19 | 1.37 | 10^{-3} | 0.07 | 3.80 | 10^{-5} | 0.12 | 0.17 | 0.12 | 0.14 |
| 1.25 | 1.31 | 2.17 | 10^{-3} | 0.10 | 5.56 | 10^{-5} | 0.19 | 0.28 | 0.19 | 0.21 |
| 1.50 | 1.46 | 3.12 | 10^{-3} | 0.15 | 7.38 | 10^{-5} | 0.27 | 0.43 | 0.27 | 0.31 |
| 1.75 | 1.68 | 4.40 | 10^{-3} | 0.20 | 8.93 | 10^{-5} | 0.36 | 0.63 | 0.37 | 0.42 |
| 2.00 | 1.98 | 5.90 | 10^{-3} | 0.26 | 9.89 | 10^{-5} | 0.47 | 0.89 | 0.48 | 0.55 |
| 2.25 | 2.45 | 7.55 | 10^{-3} | 0.32 | 1.01 | 10^{-4} | 0.57 | 1.22 | 0.60 | 0.69 |
| 2.50 | 3.30 | 9.30 | 10^{-3} | 0.38 | 0.94 | 10^{-4} | 0.67 | 1.66 | 0.75 | 0.86 |
| 2.75 | 5.80 | 1.10 | 10^{-2} | 0.44 | 0.84 | 10^{-4} | 0.75 | 2.22 | 0.90 | 1.04 |

Table 1. Properties of $n = 3/2$ polytropic model (41) with j -const rotation law and $A = 0.2R_0$. C is calculated from eq. (25) and \mathcal{C} from eq. (31). Virial test in the latter case is labeled by \mathcal{F} . By little change from \mathcal{C} to C one can notice significant improvement of virial test. In both cases virial test suggest strong deviation from equilibrium, especially for strong rotation. Actually, virial test is very sensitive to C, cf. Fig. 2. We can require virial theorem to be satisfied, by use of another value for C, solution of eq. (35). Results can be improved significantly this way – compare with Table 2 and Fig. 5.

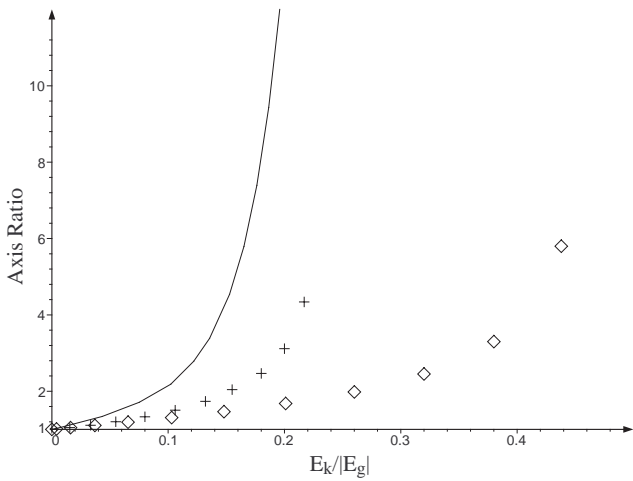


Figure 6. Axis ratio versus $E_k = E_g j$. We see that our formula (+ ; \diamond) underestimates axis ratio. Choose of C satisfying virial theorem (+) improves situation a bit. Solid line again is result of (Eriguchi & Müller 1985).

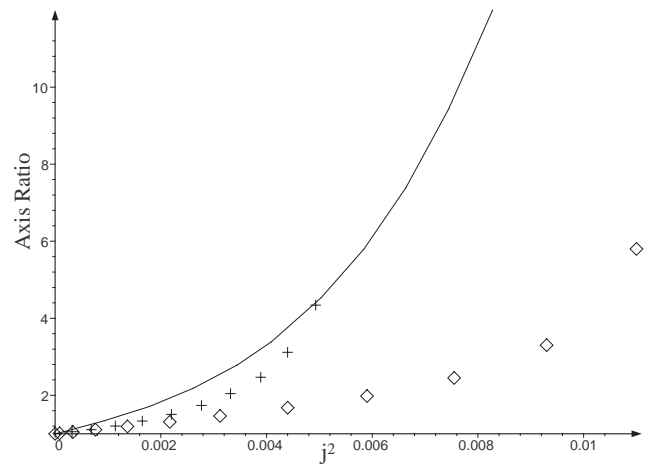


Figure 7. Axis ratio vs j^2 . Everything the same as in Fig. 6. C from eq. (33) (+) gives better approximation to axis ratio compared to formula (25) (\diamond).

underestimated, even for small values of j^2 . Fig. 6 and Fig. 7 show minor improvements when we use C from virial test (35) instead of mean value (25).

This subsection clearly show importance of constant value C. Best results are produced with C from eq. (35), therefore this value will be used in the next subsections to investigate influence of differential rotation parameter A and type of rotation law on formula accuracy.

5.2 Effects of differential rotation

In addition to the results from previous subsection (j -const with $A = 0.2R_0$) we have calculated properties of the almost rigidly ($A = 2R_0$) and extremely differentially ($A = 0.02R_0$) rotating model with the same rotation law.

In all three cases we are able to find value of C satisfying eq. (35). However, this is not enough to find correct solution, because other parameters describing rotating body may be wrong. This is clearly shown on Fig. 9, where $E_k = E_g$ versus j^2 (45) is plotted for three cases of differential rotation. Apparent discrep-

ancy for $A = 2R_0$ exists. Both j -const and v -const angular velocity profiles behaves as rigid rotation in this case. Thus we conclude that our formula is unable to predict correct structure in case of uniform rotation even if rotation is small.

If rotation is concentrated near rotation axis, like in $A = 0.02R_0$ case, our and numerical results are of the same order of magnitude. Quantitative agreement is achieved only for very small values of α . Let's note that in this case C required by virial theorem (35) is slightly below zero (Table 4). This example shows, that C may also be negative. All three cases are summarized on Fig. 9.

Results from this section show, that our formula is able to find correct structure of rotating body for differential rotation only. Range of application vary with differential rotation parameters, and best results are obtained in middle range i.e. $A = 0.2R_0$. With extremal case ($A = 0.02R_0$) quality of our results is significantly degraded.

In next subsection we examine, if this statement depends on rotation law.

| α | Axis Ratio | j^2 | $\frac{E_k}{E_0}$ | $\frac{E_g + E_k + U}{E_0}$ | Virial test \mathcal{J} | C |
|----------|------------|-------------------|-------------------|-----------------------------|---------------------------|-------|
| 0.25 | 1:01 | $8.30 \cdot 10^5$ | 0:004 | $2.05 \cdot 10^6$ | $9 \cdot 10^5$ | 0:004 |
| 0.50 | 1:05 | $3.22 \cdot 10^4$ | 0:02 | $0.98 \cdot 10^5$ | $3 \cdot 10^4$ | 0:02 |
| 0.75 | 1:11 | $6.86 \cdot 10^4$ | 0:03 | $2.10 \cdot 10^5$ | $3 \cdot 10^5$ | 0:04 |
| 1.00 | 1:20 | $1.14 \cdot 10^3$ | 0:06 | $3.50 \cdot 10^5$ | $4 \cdot 10^5$ | 0:08 |
| 1.25 | 1:33 | $1.65 \cdot 10^3$ | 0:08 | $5.14 \cdot 10^5$ | $6 \cdot 10^4$ | 0:13 |
| 1.50 | 1:51 | $2.20 \cdot 10^3$ | 0:11 | $6.84 \cdot 10^5$ | $4 \cdot 10^4$ | 0:19 |
| 1.75 | 1:74 | $2.77 \cdot 10^3$ | 0:13 | $8.55 \cdot 10^5$ | $3 \cdot 10^5$ | 0:27 |
| 2.00 | 2:04 | $3.32 \cdot 10^3$ | 0:16 | $1.00 \cdot 10^4$ | $1 \cdot 10^3$ | 0:37 |
| 2.25 | 2:47 | $3.89 \cdot 10^3$ | 0:18 | $1.18 \cdot 10^4$ | $9 \cdot 10^4$ | 0:48 |
| 2.50 | 3:12 | $4.40 \cdot 10^3$ | 0:20 | $1.33 \cdot 10^4$ | $3 \cdot 10^4$ | 0:62 |
| 2.75 | 4:34 | $4.93 \cdot 10^2$ | 0:22 | $1.50 \cdot 10^4$ | $1 \cdot 10^6$ | 0:77 |

Table 2. The same model as in Table 1, but now C is derived numerically from eq. (35). Virial test show accuracy of solution to eq. (35). Comparison with Table 1 and Table 1b of Eriguchi & Müller (1985) shows significant improvement of the total energy. Axis ratio is also closer to results of numerical calculations, and stability indicator $E_k = \mathcal{E}_g j$ isn't unreasonably high. See also Figs 4–7.

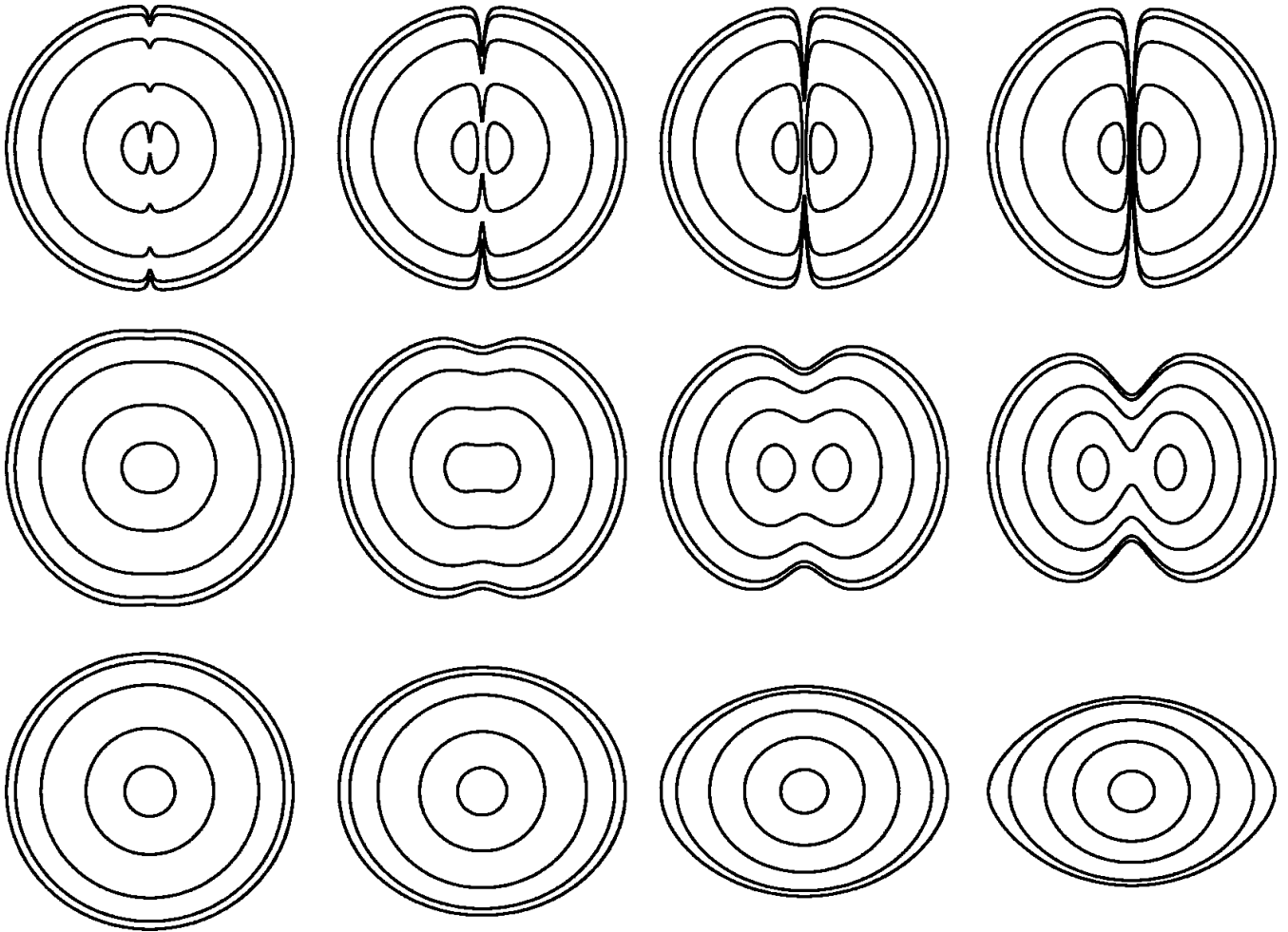


Figure 8. Examples of the density distributions given by our formula (41). Results for polytropic model with $\gamma = 5/3$ and so-called j -const (Eriguchi & Müller 1985) rotation law $\omega(r) = \omega_0(1 + r^2/A^2)$ are presented. Upper row corresponds to differential rotation with $A = 0.02R_0$. The value of α increases from left to the right. Lower row shows behaviour of the almost rigidly rotating star with $A = 2R_0$. For the middle row $A = 0.2R_0$ is adopted. R_0 is the radius of non-rotating star. Values of the α are, from left: upper row 75, 150, 200, 250; middle row 0.5, 1.0, 1.5, 2.0; bottom row 0.01, 0.02, 0.03, 0.035. Constant C is calculated from eq. (31).

| α | Axis Ratio | j^2 | $\frac{E_k}{E_g}$ | $\frac{E_g + E_k + U}{E_0}$ | Virial test χ_j | C |
|----------|------------|-------------|-------------------|-----------------------------|----------------------|------|
| 0:01 | 1:04 | 6:10 10^6 | 1:9 10^4 | 1:83 10^7 | 9 10^5 | 0:01 |
| 0:02 | 1:20 | 2:96 10^5 | 8:7 10^4 | 8:80 10^7 | 1 10^4 | 0:06 |
| 0:03 | 1:84 | 1:26 10^4 | 2:9 10^3 | 3:58 10^6 | 5 10^4 | 0:15 |
| 0:035 | 2:30 | 4:49 10^4 | 7:0 10^3 | 1:13 10^5 | 3 10^5 | 0:24 |

Table 3. Properties of our approximate sequence in case of j -const rotation law with $A = 2R_0$, i.e. almost uniform rotation. In spite of fact that virial test is fulfilled with accuracy of order 10^{-4} , comparison of data in this table with numerical results (cf. Fig. 9) clearly shows that our formula fails in case of rigid rotation.

| α | Axis Ratio | j^2 | $\frac{E_k}{E_g}$ | $\frac{E_g + E_k + U}{E_0}$ | Virial test χ_j | C |
|----------|------------|-------------|-------------------|-----------------------------|----------------------|------|
| 25 | 1:01 | 1:45 10^4 | 0:02 | 0:44 10^5 | 4 10^4 | 0:01 |
| 50 | 1:05 | 4:73 10^4 | 0:07 | 1:42 10^5 | 3 10^4 | 0:02 |
| 75 | 1:12 | 8:31 10^4 | 0:12 | 2:47 10^5 | 4 10^4 | 0:03 |
| 100 | 1:23 | 1:17 10^3 | 0:16 | 3:36 10^5 | 2 10^4 | 0:02 |
| 150 | 1:55 | 1:63 10^3 | 0:23 | 4:65 10^5 | 4 10^4 | 0:07 |
| 200 | 2:06 | 1:96 10^3 | 0:28 | 5:50 10^5 | 3 10^4 | 0:24 |
| 250 | 2:95 | 2:21 10^3 | 0:32 | 6:12 10^5 | 1 10^4 | 0:49 |
| 300 | 5:76 | 2:42 10^3 | 0:34 | 6:64 10^5 | 3 10^4 | 0:83 |

Table 4. Properties of sequence with j -const rotation law for $A = 0:02R_0$.

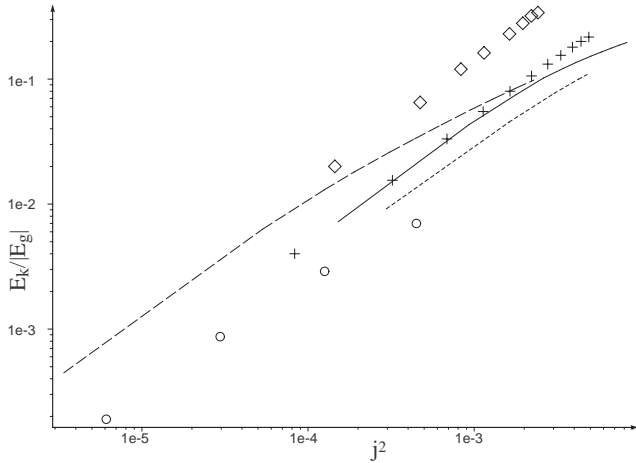


Figure 9. Stability indicator E_k/E_g vs j^2 for j -const angular velocity ($\log - \log$ plot) for three values of A . Quantitative agreement between our formula (symbols) and numerical results (Eriguchi & Müller 1985, lines) is achieved for $A = 0:02R_0$ if $E_k/E_g \ll 0:1$. This case is presented as solid line and crosses. In case of $A = 0:02R_0$ we have results of the same order, but they are identical only in case where rotation strength is very small. This case is presented by dashed line and diamonds. Formula fails (dotted line and circles) in case of rigid rotation.

5.3 Rotation law effects

In addition to previously described cases, we have calculated global properties of our model in case of v -const angular velocity profile, with parameter $A = 0:2R_0$ (Table 5) and $A = 0:02R_0$ (Table 6). Results with $A = 2R_0$ aren't presented, because they are similar to j -const case (cf. Table 3), where both functions (χ) behave as uniform rotation, and our formula fails in this case.

Figures 10 and 12 show very good agreement of the global physical quantities ($E_k/E_g; j^2; E_{\text{tot}}$) with numerical results for

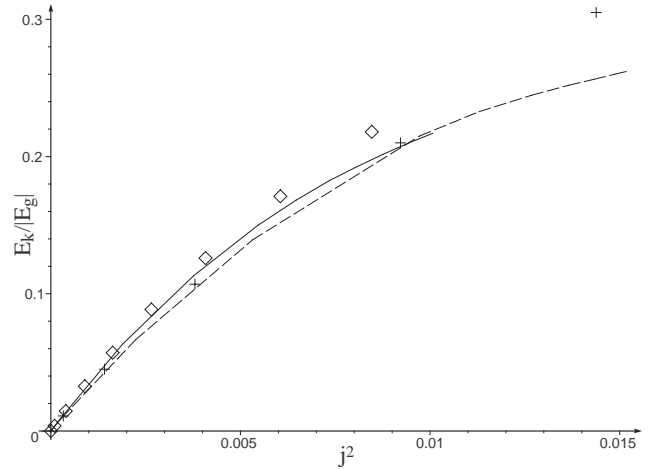


Figure 10. $E_k/E_g(j^2)$ for v -const rotation law with $A = 0:02R_0$ (dashed, cross) and $A = 0:02R_0$ (solid, diamond), where lines refers to Eriguchi & Müller (1985) and symbols refers to our formula with C from (35). In this case we have good quantitative agreement with numerical results in both cases up to $E_k/E_g \approx 0:1$.

entire range of rotation strength covered by both methods. The most extreme case ($A = 0:02$) also behaves well. Axis ratio (Fig. 13) however, clearly distinguish between approximation and precise solution. Results are quantitatively correct only for small rotation parameters, e.g. $j^2 \ll 0:005$ i.e. $E_k/E_g \ll 0:1$.

6 DISCUSSION & CONCLUSIONS

Comparison of the results obtained with our approximation formula (Fig. 11 – Fig. 13, Table 2–5) with other (Eriguchi & Müller 1985, Fig. 2–5, Fig. 9, Table 1 and 2) shows a correct qualitative

| α | Axis Ratio | j^2 | $\frac{E_k}{E_g}$ | $\frac{E_g + E_k + U}{E_0}$ | Virial test \mathcal{V} | $\mathcal{V} j$ | C |
|----------|------------|----------------------|-------------------|-----------------------------|---------------------------|-----------------|------|
| 0.25 | 1.05 | $3.29 \cdot 10^{-4}$ | 0.01 | $0.99 \cdot 10^{-5}$ | 9 | 10^{-5} | 0.01 |
| 0.50 | 1.21 | $1.41 \cdot 10^{-3}$ | 0.05 | $4.26 \cdot 10^{-5}$ | 2 | 10^{-4} | 0.05 |
| 0.75 | 1.63 | $3.80 \cdot 10^{-3}$ | 0.11 | $1.12 \cdot 10^{-4}$ | 2 | 10^{-4} | 0.13 |
| 1.00 | 2.31 | $9.22 \cdot 10^{-3}$ | 0.21 | $2.52 \cdot 10^{-4}$ | 3 | 10^{-4} | 0.27 |
| 1.25 | 5.26 | $1.44 \cdot 10^{-2}$ | 0.31 | $3.87 \cdot 10^{-4}$ | 5 | 10^{-4} | 0.47 |

Table 5. Properties of our model with v -const rotation law and $A = 0.02R_0$.

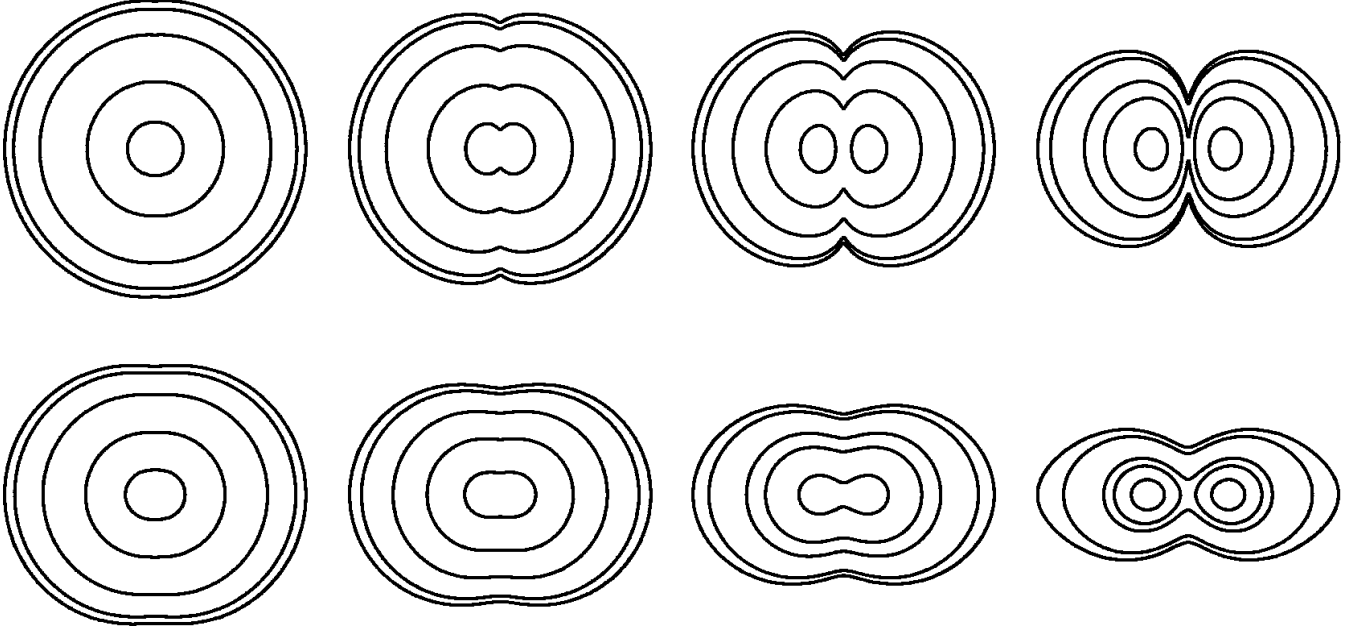


Figure 11. Another example of density distributions given by our formula (41). The same as in Fig. 8 for so-called v -const rotation law (Eriguchi & Müller 1985) ($\alpha = \alpha_0(1 + r/A)$). Values of α_0 are, from left: in the upper ($A = 0.02R_0$) row: 1.0, 3.0, 5.0, 7.0; in the bottom ($A = 0.02R_0$) row: 0.5, 0.75, 1.0 and 1.25.

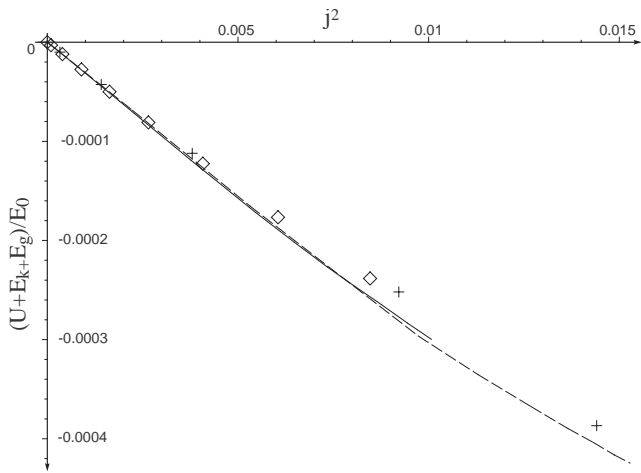


Figure 12. E_{tot} versus square of dimensionless angular momentum j^2 . Symbols description is the same as on previous figure, Fig. 10.

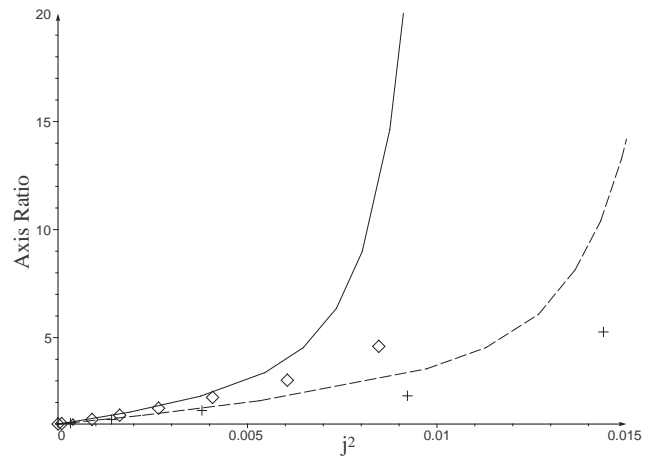


Figure 13. Axis ratio versus j^2 for v -const rotation law. Symbols description is the same as on previous figures, Fig. 10 and Fig. 12.

behaviour for even the most simplified version of our approximation formula for a wide range of parameters describing differential rotation and strength of rotation. This makes our formula an excellent tool for those who are interested in the structure of barotropic,

differentially rotating stars, but do not need exact, high precision results. It can be applied for qualitative analysis of structure of rapidly rotating stellar cores (e.g. ‘cusp’ formation, degree of flattening, off-centre maximum density) with arbitrary rotation

| α | Axis Ratio | j^2 | $\frac{E_k}{E_g j}$ | $\frac{E_g + E_k + U}{E_0}$ | Virial test $\mathcal{Z} j$ | C |
|----------|------------|-------|---------------------|-----------------------------|-----------------------------|------|
| 1:0 | 1:02 | 9:81 | 10^{-5} | 0:004 | 0:30 10^{-5} | 0:01 |
| 2:0 | 1:09 | 3:94 | 10^{-4} | 0:015 | 1:20 10^{-5} | 0:04 |
| 3:0 | 1:21 | 8:96 | 10^{-4} | 0:03 | 2:75 10^{-5} | 0:09 |
| 4:0 | 1:41 | 1:63 | 10^{-3} | 0:06 | 5:00 10^{-5} | 0:17 |
| 5:0 | 1:73 | 2:65 | 10^{-3} | 0:09 | 8:09 10^{-5} | 0:27 |
| 6:0 | 2:24 | 4:08 | 10^{-3} | 0:13 | 1:23 10^{-4} | 0:39 |
| 7:0 | 3:03 | 6:05 | 10^{-3} | 0:17 | 1:77 10^{-4} | 0:55 |
| 8:0 | 4:60 | 8:46 | 10^{-3} | 0:22 | 2:38 10^{-4} | 0:75 |

Table 6. Properties of v -const sequence for $\Lambda = 0:02R_0$.

law, also for initial guess for numerical algorithms. It can also be used as an alternative for high-quality numerical results for use in a more convenient form as long as $E_k = \mathcal{E}_g j^{-2} < 0.1$ and we are interested mainly in global properties of differentially rotating objects.

ACKNOWLEDGMENTS:

I would like to thank Prof. K. Grotowski and M. Misiaszek for thorough discussion of the problem, and Prof. M. Kutschera for critical reading of the previous version of this article.

REFERENCES

- Chandrasekhar, S. 1936 MNRAS, 93, 390
 Eriguchi, Y. and Müller, E. 1985 A&A, 146, 260
 Hachisu, I. 1986 ApJS, 61, 479
 Hammerstein, A. 1930 Acta Mathematica, 54, 117
 Kippenhahn, R., Weigert, A., 1994, Stellar Structure and Evolution. Springer-Verlag p. 176
 Lyttleton, R.A., 1953, The Stability of Rotating Liquid Masses. Cambridge University Press
 Maclaurin, C., 1742, A treatise of fluxions. Printed by T. W. & T. Ruddimans, Edinburg
 Ostriker, J.P., Mark, J.W.-K. 1968 ApJ, 151, 1075
 Tassoul, J.-L., 2000, Stellar Rotation. Cambridge University Press p. 56